View Article Online / Journal Homepage / Table of Contents for this issue

Two polyaminophenolic fluorescent chemosensors for H^+ and Zn(II). Spectroscopic behaviour of free ligands and of their dinuclear Zn(II) complexes†

Gianluca Ambrosi,[a] Cristina Battelli,[a] Mauro Formica,[a] Vieri Fusi,*[a] Luca Giorgi,[a] Eleonora Macedi,[a] Mauro Micheloni,*[a] Roberto Pontellini[a] and Luca Prodi[b]

Received (in Durham, UK) 17th June 2008, Accepted 18th September 2008
First published as an Advance Article on the web 31st October 2008
DOI: 10.1039/b810228g

Published on 31 October 2008 on http://pubs.rsc.org | doi:10.1039/B810228G
Downloaded on 02 January 2013

The UV-Vis and fluorescence optical properties of the two polyamino-phenolic ligands 3,3′-bis[*N*,*N*-bis(2-aminoethyl)aminomethyl]-2,2′-dihydroxybiphenyl (**L1**) and 2,6-bis{[bis-(2-aminoethyl)amino]methyl}phenol (**L2**) were investigated in aqueous solution at different pH values as well as in the presence of Zn(II) metal ion. Both ligands show two diethylenetriamine units separated by the 1,1′-bis(2-phenol) (BPH) or the phenol (PH) for **L1** and **L2**, respectively. Both ligands are fluorescence-emitting systems in all fields of pH examined, with **L1** showing a higher fluorescence emission than **L2**. In particular, the emission of fluorescence mainly depends on the protonation state of the phenolic functions and thus on pH. The highest emitting species is H_3L^{3+} for both systems, where the BPH is monodeprotonated (in **L1**) and the PH is in the phenolate form (in **L2**). On the contrary, when BPH and PH are in their neutral form both ligands show the lowest fluorescence, since H-bonds occurring between the phenol and the closest tertiary amine functions decrease fluorescence. The Zn(II)-dinuclear species are also fluorescent in the pH range where they exist; the highest emitting species being $[Zn_2(H_{-2}\mathbf{L1})]^{2+}$ and $[Zn_2(H_{-1}\mathbf{L2})]^{3+}$ which are present in a wide range of pH including the physiological one. Fluorescence experiments carried out at physiological pH highlighted that, in the case of **L1**, the presence of Zn(II) ion in solution produces a simultaneous change in λ_{em} with a drop in fluorescence due to the formation of the $[Zn_2(H_{-2}\mathbf{L1})]^{2+}$ species, while, in the case of **L2**, it gives rise to a strong CHEF effect (a twenty-fold enhancement was observed) due to the formation of the $[Zn_2(H_{-1}\mathbf{L2})]^{3+}$ species. These results, supported by potentiometric, ^1H and ^{13}C NMR experiments, are of value for the design of new efficient fluorescent chemosensors for both H^+ and Zn(II) ions.

Introduction

The development of chemosensors is in continuous expansion due to their usefulness in many fields; they have a wide range of applications, such as environmental monitoring, process control, food and beverage analysis, medical diagnosis and others.[1–8] Due to their use in many disciplines, they are very attractive for chemists, biologists, physicists and material scientists. For example, in biochemistry, clinical and medical sciences, and cell biology, freely mobile sensor molecules are employed extensively in microscopy, offering the possibility of performing real-space measurements.[9,10]

Among the different chemosensors, the fluorescence-based ones present many advantages: fluorescence measurements are usually very sensitive, low-cost, easily performed and versatile, offering submicrometer spatial resolution and submillisecond temporal resolution.[11–19] The versatility of fluorescence-based sensors originates also from the wide number of parameters that can be tuned in order to optimize the convenient signal. In most cases, changes in luminescence intensity represent the most directly detectable response to target recognition; more recently, however, other properties such as excited-state lifetime and fluorescence anisotropy have also been preferred as diagnostic parameters, since they are less affected by environmental and experimental conditions.

Phenol and poly-phenols show well known optical properties which mainly depend on their protonation degree;[20,21] in our lab, several polyamino-phenolic ligands of different topologies have been synthesized. In this study, we wanted to extend our knowledge to the spectroscopic properties of two of them to identify their possible applications as chemosensors for suitable guests. In this case, we focused our attention on the two previously synthesized amino-phenolic ligands **L1** and **L2** (Chart 1). They were chosen for several reasons: they have similar topology; they both show two diethylenetriamine (dien) units separated by a phenolic aromatic spacer, the 1,1′-bis(2-phenol) group (BPH) and the phenol for **L1** and

[a] *Institute of Chemical Sciences, University of Urbino, P.za Rinascimento 6, I-61029 Urbino, Italy*
[b] *Department of Chemistry, University of Bologna, Via Selmi 2, Bologna, Italy. E-mail: vieri@uniurb.it*
† Electronic supplementary information (ESI) available: Fig. S1: Location of acidic hydrogen atoms in the protonated species of **L2**. See DOI: 10.1039/b810228g

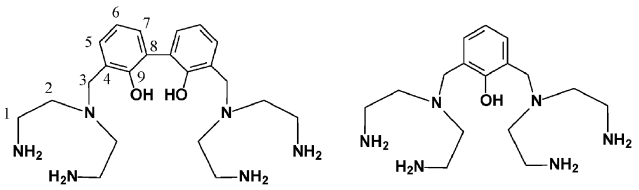

Chart 1 Ligands together with labels for the NMR resonances.

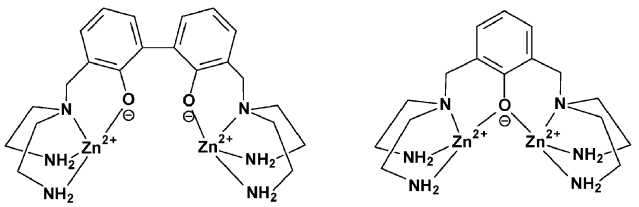

Scheme 1 Coordination scheme for Zn(II) in the $[Zn_2(H_{-2}\mathbf{L1})]^{2+}$ and $[Zn_2(H_{-1}\mathbf{L2})]^{3+}$ complexes.

L2, respectively; in addition, they easily form dinuclear species with transition metal ions. The molecular skeleton of both ligands affords the formation of preorganized dinuclear Zn(II) species where the two Zn(II) ions can cooperate in binding guests; in particular, it has been demonstrated that in some dinuclear species such as the $[Zn_2(H_{-2}\mathbf{L1})]^{2+}$ and $[Zn_2(H_{-1}\mathbf{L2})]^{3+}$ ones, the two zinc ions show, in both systems, an equal coordination environment, are displaced at fixed different distances and are able to add guests to saturate the coordination requirement of the two zinc ions (see Scheme 1).

Although zinc is an essential metal ion in human life and plays a fundamental role in many biological functions, for example in the alkaline phosphatase or carbonic anhydrase enzymes,[22] excess zinc can be very harmful, as it can lead to many health problems.[23] For this reason, easy recognition of the zinc ion is key mainly and as a result many fluorescent molecular sensors have been developed in recent years, also to allow its *in vivo* mapping.[24]

In this work, we have studied the NMR, UV-Vis and fluorescence properties of the free ligands as well as of their zinc complexes in aqueous solution. The aim has been to detect if the optical properties of these systems are affected by pH as well as by the presence of Zn(II) in solution.

Experimental

Synthesis

Ligand 3,3′-bis[*N*,*N*-bis(2-aminoethyl)aminomethyl]-2,2′-dihydroxybiphenyl (**L1**) and 2,6-bis{[bis-(2-aminoethyl)amino]-methyl}phenol (**L2**) were prepared as previously described.[25]

EMF measurements

Equilibrium constants for protonation and complexation reactions with **L2** were determined by pH-metric measurements ($pH = -\log[H^+]$) in 0.15 M NaCl at 298.1 ± 0.1 K, using the fully automatic equipment that has already been described; the EMF data were acquired with the PASAT computer program.[26] The combined glass electrode was calibrated as a hydrogen concentration probe by titrating known amounts of HCl with CO_2-free NaOH solutions and determining the equivalent point by Gran's method,[27] which gives the standard potential E° and the ionic product of water (pK_w = 13.73(1) at 298.1 K in 0.15 M NaCl, $K_w = [H^+][OH^-]$). At least three potentiometric titrations were performed for each system in the pH range 2–11, using different molar ratios of Zn(II)/**L2** ranging from 1:1 to 2:1. All titrations were treated either as single sets or as separate entities, for each system; no significant variations were found in the values of the determined constants. The HYPERQUAD computer program was used to process the potentiometric data.[28]

Spectroscopic experiments

^1H and ^{13}C NMR spectra were recorded on a Bruker Avance 200 instrument, operating at 200.13 and 50.33 MHz, respectively, and equipped with a variable temperature controller. The temperature of the NMR probe was calibrated using 1,2-ethanediol as calibration sample. For the spectra recorded in D_2O, the peak positions are reported with respect to HOD (4.75 ppm) for ^1H NMR spectra, while dioxane was used as reference standard in ^{13}C NMR spectra (δ = 67.4 ppm). Fluorescence spectra were recorded at 298 K with a Varian Cary Eclipse spectrofluorimeter. UV absorption spectra were recorded at 298 K with a Varian Cary-100 spectrophotometer equipped with a temperature control unit.

The fluorescence quantum yields (Φ_f) of the highest fluorescent species were calculated as reported in ref. 29 using 2-aminopyridine as standard reference.

Results and discussion

Solution studies

Ligands **L1** and **L2** as well as the Zn(II)/L systems were studied by fluorescence spectroscopy in aqueous solution at different pH values to investigate the fluorescence properties of both ligands and how these are affected by protonation and the presence of Zn(II) ion. ^1H and ^{13}C NMR experiments on the free **L1** as well as those reported for the Zn(II)/**L1** system[25a] aided in understanding the role played by both protonation and Zn(II). The fluorescence quantum yields (Φ_f) of the highest fluorescent species are reported in Table 1.

Similar ^1H NMR studies carried out on **L2** and Zn(II)/**L2** system are reported in refs. 30 and 31, respectively. Moreover, further studies on the UV-Vis absorption properties of both L and Zn(II)/L systems were performed in aqueous solution in addition to those already reported.[25,30,31]

Table 1 Fluorescence quantum yield (Φ_f) of the main fluorescent species in 0.15 mol dm^{-3} NaCl at 298.1 K

	Φ_f
$H_3\mathbf{L1}^{3+}$	0.34
$H_3\mathbf{L2}^{3+}$	0.01
$[Zn_2H_{-2}\mathbf{L1}]^{2+}$	0.24
$[Zn_2H_{-1}\mathbf{L2}]^{3+}$	0.08

Published on 31 October 2008 on http://pubs.rsc.org | doi:10.1039/B810228G
Downloaded on 02 January 2013

 This journal is © The Royal Society of Chemistry and the Centre National de la Recherche Scientifique 2009

Published on 31 October 2008 on http://pubs.rsc.org | doi:10.1039/B810228G
Downloaded on 02 January 2013

L1 and L2 in aqueous solution at different pH values

Basicity. The basicity of **L1** in 0.15 mol dm^{-3} NaCl aqueous solution at 298.1 K was potentiometrically studied and the results obtained reported in ref. 25*a*; the protonation constants of ligand **L2** were determined under these ionic conditions and the stepwise basicity constants of **L2** are reported in Table 2. The basicity of **L2** is similar to that previously reported using NMe_4Cl as ionic medium thus the discussion can be outlined in the same way.[30]

Fluorescence of L1 at different pH values. Emission spectra performed at different pH values gave information on the interaction between the dien and the 2,2′-biphenol (BPH) units and on the behavior of the ligand in its excited states.

As reported in the literature, BPH shows emission of fluorescence depending on the degree to which it is deprotonated;[20] in particular, it shows the most intense fluorescence in its monodeprotonated form and the least intense in its neutral one (more than six times lower), while the dianionic form, although fluorescent, is obtainable only at very high pH values (pH > 15).[20,32]

Table 2 Basicity and equilibrium constants for the complexation reactions of **L2** with Zn(II) ion determined in 0.15 mol dm^{-3} NaCl at 298.1 K

Reaction	log K
$L + H^+ = HL^+$	10.04(1)[a]
$HL^+ + H^+ = H_2L^{2+}$	9.87(1)
$H_2L^{2+} + H^+ = H_3L^{3+}$	9.12(1)
$H_3L^{3+} + H^+ = H_4L^{4+}$	7.59(1)
$H_4L^{4+} + H^+ = H_5L^{5+}$	2.50(3)
$Zn^{2+} + L + 2H^+ = ZnH_2L^{4+}$	28.42(1)
$Zn^{2+} + L + H^+ = ZnHL^{3+}$	23.82(2)
$Zn^{2+} + L = ZnL^{2+}$	14.67(2)
$Zn^{2+} + L = Zn(H_{-1}L)^+ + H^+$	5.05(2)
$2Zn^{2+} + L = Zn_2(H_{-1}L)^{3+} + H^+$	17.17(1)
$2Zn^{2+} + L + H_2O = Zn_2(H_{-1}L)OH^{2+} + 2H^+$	8.34(3)
$2Zn^{2+} + L + 2H_2O = Zn_2(H_{-1}L)(OH)_2^+ + 3H^+$	−1.63(3)
$Zn_2(H_{-1}L)^{3+} + OH^- = Zn_2(H_{-1}L)OH^{2+}$	4.90
$Zn_2(H_{-1}L)OH^{2+} + OH^- = Zn_2(H_{-1}L)(OH)_2^+$	3.76

[a] Values in parentheses are the standard deviations on the last significant figure.

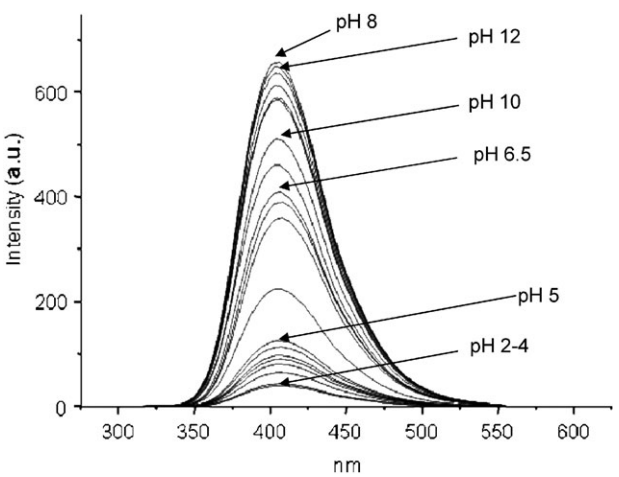

Fig. 1 Fluorescence spectra of **L1** at different pH values.

The fluorescence spectra of **L1** (λ_{exc} = 287 nm) recorded in aqueous solution in the pH range 2–12 are reported in Fig. 1; the trend of the fluorescence emission intensity (◆) *vs.* pH (λ_{exc} = 287 nm) is reported in Fig. 2(a) together with the maximum absorption (···) and the emission (---) wavelength trend. Fig. 2(b) reports the trend of the absorption titration at λ = 308 nm (●) together with the distribution curves for the species of **L1** (—) as a function of pH.

Excitation of **L1** acid solution at pH 2 (λ_{exc} = 287 nm) gives rise to a fluorescence emission band of very low intensity (λ_{em} = 403 nm) attributed to the BPH fluorophore. The intensity of the fluorescence emission of the compound is highly dependent on the protonation state of the ligand (see Fig. 1 and 2(a)); however the shape and the λ_{em} of the spectra are substantially pH-independent. In this pH range, the free BPH group shows a similar fluorescent behavior produced by the monoanionic excited state of BPH.[20,32] Taking into account that the fluorescence of **L1** is due to the BPH fluorophore, this suggests that also in **L1** the changes in fluorescence emission reflect only the ground states acid–base equilibrium.[33] For this reason, no indication of the excited state proton transfer reaction was found and, as reported for free BPH, the fluorescence is due to the monoanionic excited state of BPH in **L1**.

In the fluorescence spectra, the emission remains substantially very low and constant (Fig. 2(a)) at acidic pH values (2 ≤ pH ≤ 5) while it starts increasing at pH 5 in concomitance with the appearance of the $H_3\mathbf{L1}^{3+}$ species in solution, reaching a maximum intensity at pH 7.4–8.4 with the complete formation of the $H_3\mathbf{L1}^{3+}$ species. A small decrease can be

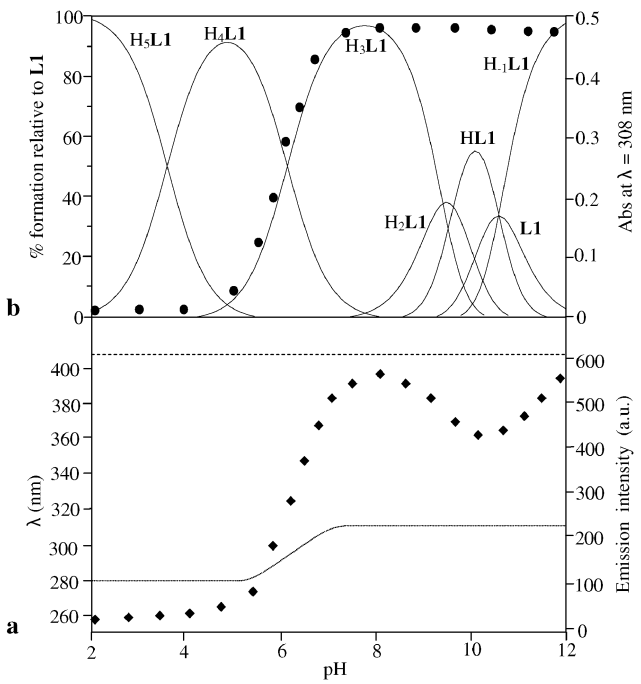

Fig. 2 Fluorescent emission titration (λ_{exc} = 287 nm, λ_{em} = 403 nm) (◆), absorption wavelength trend (···), and emission wavelength trend (---) (a); absorption titration at λ = 308 nm (●) and distribution curves of the species (—) (b) as function of pH in aqueous solution: [**L1**] = 5.0 × 10^{-5} M, I = 0.15 M NaCl, T = 298.1 K.

Published on 31 October 2008 on http://pubs.rsc.org | doi:10.1039/B810228G
Downloaded on 02 January 2013

observed in the alkaline range up to pH 10.5 at which the less protonated species appear in solution; on the contrary, when the pH is increased to 11 emission rises again, reaching maximum intensity at pH 12 with the presence in solution of the monoanionic $H_{-1}\mathbf{L1}^{-}$ species.

Bearing in mind the previous studies on BPH,[20,32] the trend of the emission intensity in the range of pH 2–8 can be easily explained by the deprotonation of the neutral BPH unit to form its monoanionic species that occurs with the formation of the $H_3\mathbf{L1}^{3+}$ species. In other words, in the protonated species $H_5\mathbf{L1}^{5+}$ and $H_4\mathbf{L1}^{4+}$, BPH is present in its neutral form while in the $H_3\mathbf{L1}^{3+}$ species it has lost one of the acidic protons forming the highest emitting species (Φ = 0.34, Table 1). These results are in agreement with those already obtained by UV-Vis absorption studies which revealed that the deprotonation of one of the hydroxyl functions of BPH occurred in the pH range involving the passage from $H_4\mathbf{L1}^{4+}$ to $H_3\mathbf{L1}^{3+}$ species.[25a] This was highlighted, as reported in Fig. 2(b), by the change in absorption at 308 nm which increases when the monoanionic form of BPH is present in solution and is further underlined by the variation in the trend of the maximum of the absorption wavelength (Fig. 2(a)) as a function of pH; both figures highlight that the changes take place in the field of pH where the $H_3\mathbf{L1}^{3+}$ species forms. Although the absorption and emission wavelength maxima as well as the absorption at 308 nm remain constant, increasing the pH to form lesser protonated species than $H_3\mathbf{L1}^{3+}$, there is a small decrease (about 25% at pH 10) in fluorescence intensity occurring with the formation of the $H_2\mathbf{L1}^{2+}$, $H\mathbf{L1}^{+}$ and neutral **L1** species (Fig. 2(a)). This trend could be explained by the formation of a H-bond network involving BPH and the closer nitrogen atoms. In fact, as reported for free BPH,[20,32] the formation of an intramolecular H-bond interaction occurring between the two oxygen atoms of BPH in stabilizing the hydrogen atom in the monoanionic species gives the greatest fluorescence intensity, while, on the contrary, the formation of intermolecular H-bonds with H-accepting molecules, such as water, gives rise to a very fast nonradiating process throughout the H-bond, thus leading to a decrease in the fluorescence (this occurs for example in the neutral form of excited BPH). In addition, it has been demonstrated that in the presence of strong proton-accepting molecules such as triethylamine (TEA), the formation of H-bonding between TEA and a hydrogen atom of BPH once again leads to a decrease in fluorescence.[20b] In our case, it is presumable that similar H-bonding between the BPH oxygen and the closer nitrogen atoms of the dien units is formed, thus decreasing fluorescence; however, the formation of this type of H-bond cannot be the favourite situation since only a slight drop in fluorescence was observed. Moreover, two different H-bonds could be suggested in the case of **L1**: *via* OH···N as well as *via* $O^{-}\cdots HN^{+}$; in other words, in the $H_2\mathbf{L1}^{2+}$, $H\mathbf{L1}^{+}$ and **L1** species, a partial stabilization of the acidic hydrogen atom of the monoanionic BPH unit could also take place with the closer N atom (**c** in Scheme 2), but also a partial ammonium character of the closer N atom could give rise to the same quenching H-bond effect with the BPH unit (**b** in Scheme 2). In any case, the form (**a**) shown in Scheme 2 is the favoured form and it is the only one present in the $H_3\mathbf{L1}^{3+}$ as well as in the $H_{-1}\mathbf{L1}^{-}$ species where the highest fluorescence is reached. In addition, the absence of fluorescence changes even at highly alkaline pH values once again demonstrates that the full deprotonation of BPH in **L1** is not reachable under our experimental conditions.

L1 ^{1}H and ^{13}C NMR studies at different pH values. In order to obtain further structural information about the distribution of acidic protons in the protonated species of **L1**, ^{1}H and ^{13}C NMR spectra were recorded over the pH range of the

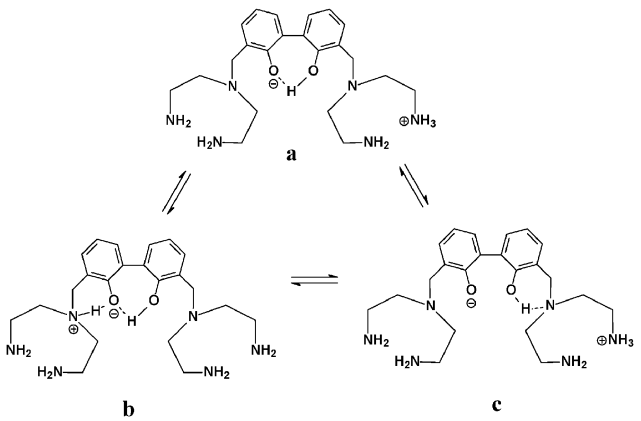

Scheme 2 Possible H-bond interactions for the neutral **L1** species.

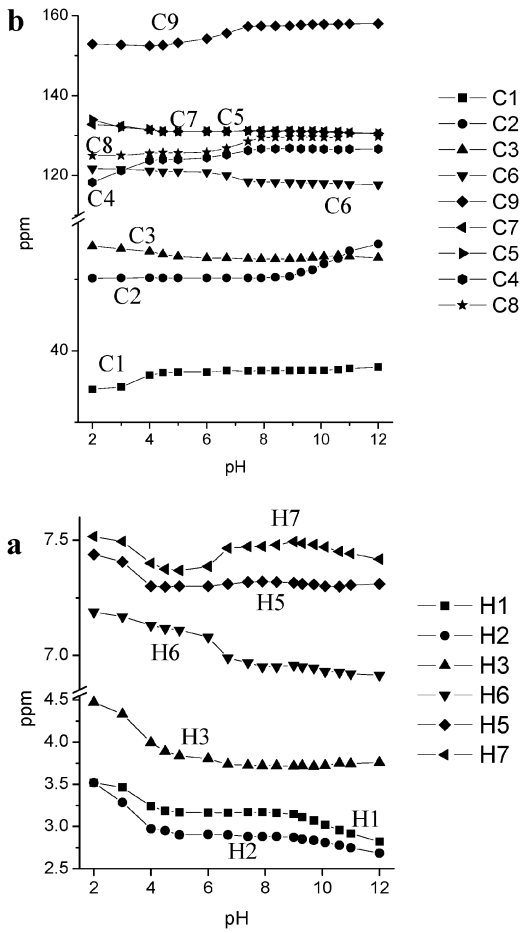

Fig. 3 Experimental NMR chemical shifts in aqueous solution of **L1** as a function of pH: ^{1}H NMR (a); ^{13}C NMR (b).

 This journal is © The Royal Society of Chemistry and the Centre National de la Recherche Scientifique 2009

Published on 31 October 2008 on http://pubs.rsc.org | doi:10.1039/B810228G
Downloaded on 02 January 2013

potentiometric, UV-Vis and fluorescence measurements. ^{1}H–^{1}H and ^{1}H–^{13}C NMR 2D correlation experiments were performed to assign all the signals. The trends for the chemical shift of the ^{1}H and ^{13}C NMR resonances are reported in Fig. 3(a) and (b). The ^{1}H NMR spectrum recorded at pH 12, where the $H_{-1}\mathbf{L1}^{-}$ species is prevalent in solution, exhibits two triplets at 2.67 and 2.85 ppm corresponding to the resonance of the hydrogen atoms H2 and H1, respectively, one singlet at 3.76 ppm due to the hydrogen atoms H3, one triplet at 6.91 ppm for the resonances of H6 and two doublets at 7.31 and 7.42 ppm for H5 and H7, respectively. This spectral feature indicates a C_{2v} symmetry mediated on the NMR time-scale which is preserved throughout the pH range investigated. In agreement with this symmetry, the ^{13}C NMR spectrum recorded at the same pH value shows only nine signals at δ 37.7 (C1), 53.0 (C3), 55.0 (C2), 117.8 (C6), 126.6 (C4), 129.7 (C8), 130.5 (C5), 130.6 (C7) and 158.0 (C9). At lower pH, where the species **L1**, $H\mathbf{L1}^{+}$, $H_2\mathbf{L1}^{2+}$ and $H_3\mathbf{L1}^{3+}$ are forming (pH = 11–7), the main shift is exhibited by the protons H1 which show a marked downfield shift, suggesting that the four protonation steps take place mainly on the primary amine functions. This hypothesis is confirmed by the trend of the ^{13}C NMR resonances which mainly shows an upfield shift in the signal of the carbon atom C2, in agreement with the β-effect of the protonation of the polyamines.[34] However, in this pH range, slight shifts in other ^{1}H NMR resonances could be seen: for example, the resonance of H7 first moves downfield up to pH 9 then decreases with the formation of the $H_3\mathbf{L1}^{3+}$ species, while H3 moves upfield; this suggests little changes in charge density on both the tertiary amine groups and BPH unit occurring in this pH range that can be correlated with the formation of H-bonding involving the BPH oxygen and the closer nitrogen atoms in the **L1**, $H\mathbf{L1}^{+}$ and $H_2\mathbf{L1}^{2+}$ species, in agreement with the fluorescence experiments reported above.

In the pH range 4–6 the $H_4\mathbf{L}^{4+}$ species is prevalent and, as demonstrated both by UV and fluorescence experiments, the fifth protonation step occurs at the BPH group. This was also confirmed in the NMR experiments by the downfield shift of the H6 signal in the *para* position to the phenolic oxygens and by the upfield shift of the H7 protons in the ^{1}H NMR spectra, as well as by the accompanying upfield shift of C4, C8 and C9 and downfield shift of C6 in the ^{13}C NMR spectra. The strong upfield shift exhibited by the signal of H7 could be related not only to a protonation process of the BPH unit but also to a change in the angle between the two aromatic rings that probably is affected by the protonation degree of **L1** leading the formation of a new H-bond network involving the neutral BPH and the unprotonated tertiary amine functions, as depicted in Fig. 4 for the $H_4\mathbf{L1}^{4+}$ species; this almost entirely quenches the fluorescence (see above). The protonation step giving the $H_5\mathbf{L}^{5+}$ species, occurring below pH 4, basically causes a downfield shift of protons H2 and H3 together with an upfield shift in the signals of the carbon atoms C1 and C4, suggesting that it takes place on the tertiary amine groups. Once again the H7 and H5 resonances, both of which shift downfield, are perturbed by this protonation step, highlighting the formation of a H-bond network with the closer amine functions on the BPH unit different from the previous one; this

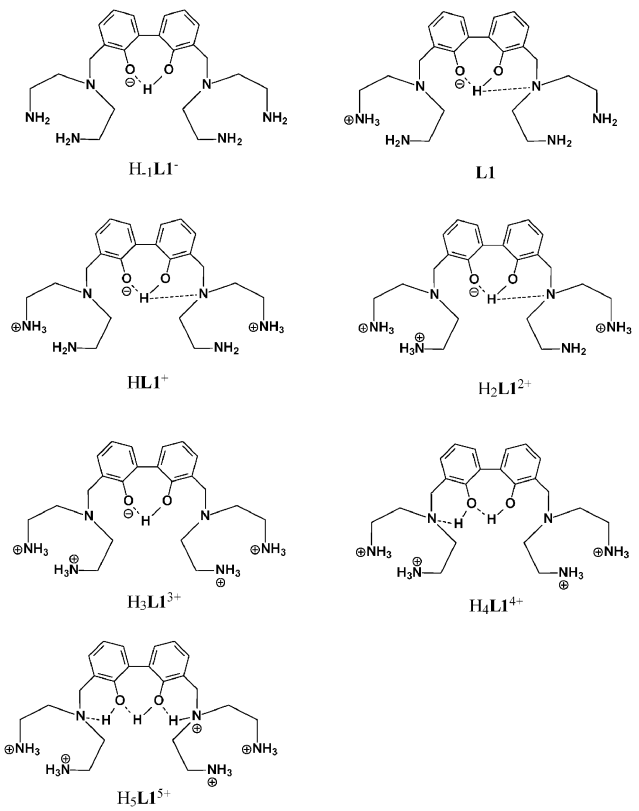

Fig. 4 Location of acidic hydrogen atoms in the protonated species of **L1**.

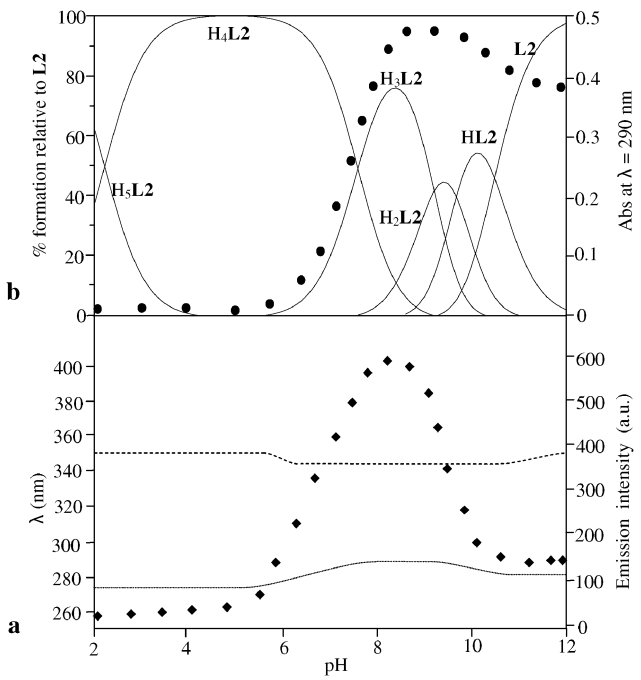

Fig. 5 Fluorescence emission titration (λ_{ex} = 280 nm) (◆), absorption wavelength trend (···), and emission wavelength trend (---) (a); absorption titration at λ = 290 nm (●) and distribution curves of the species (—) (b); of **L2** as function of pH in aqueous solution: [**L2**] = 5.0×10^{-5} M, I = 0.15 M NaCl, T = 298.1 K.

Published on 31 October 2008 on http://pubs.rsc.org | doi:10.1039/B810228G
Downloaded on 02 January 2013

affects the chemical shift, modifying the electron density of the neutral BPH unit as well as the angle between the two aromatic rings.

A protonation scheme arising from NMR experiments is summarized in Fig. 4.

Fluorescence of L2 at different pH values. The same fluorescence experiments were carried out on the ligand **L2** and compared to the previous UV-Vis and NMR studies performed in aqueous solution at different pH values.[30] The trend in fluorescence emission intensity (◆) *versus* pH (λ_{exc} = 280 nm) is reported in Fig. 5(a) together with the maximum absorption (···) and emission (---) wavelength trends. Fig. 5(b) reports the trend for the absorption titration at λ = 290 nm (●) together with the distribution curves of the species of **L2** (—) as a function of pH obtained by potentiometry.

The acidic solutions of **L2** up to pH 6 are barely fluorescent, as also reported for the free neutral phenol (PH), while fluorescence increases with the formation of the H_3**L2**$^{3+}$ species, reaching maximum emission at pH 8 together with the maximum presence in solution of the H_3**L2**$^{3+}$ species; at higher pH values, the emission drops, reaching a plateau at pH higher than 11 with the formation of the neutral **L2** species. The fluorescence of ligand **L2**, which is lower compared to that of **L1** (see Table 1), is highly dependent on the protonation state of the ligand as seen before for **L1**. The acidic proton distribution in the several protonated species of **L2** obtained by UV-Vis, potentiometry and NMR studies was previously reported and the scheme is reported in Fig. S1 of the ESI;† the most fluorescent H_3**L2**$^{3+}$ species is the one in which the phenol is deprotonated (*i.e.* phenolate) and the four acidic protons are located on the primary amine functions; this is the same situation found for the H_3**L1**$^{3+}$ species where there are no H-bond interactions with the closest amine functions, thus affording the highest emission quantum yield also in the H_3**L2**$^{3+}$ species. It should be noted that in the free PH, the anion presents a much lower fluorescence intensity than the neutral species.[21] In this case the opposite behaviour was observed; this could be explained (see also below) by a decrease in the solvation *via* H-bond network of the phenolate oxygen atom by the water molecules in the H_3**L2**$^{3+}$ species in comparison with the free PH anion.[21a] In other words, the presence of the two protonated dien units linked to the PH group modifies the accessibility of the solvent molecules to the phenolate oxygen atom decreasing its quenching effect and thus increasing the emissive relaxation decay of the PH anion. As reported, an acidic proton redistribution was observed in the less protonated species involving at least a tertiary amine function that becomes protonated. This ammonium group, found mainly in the neutral **L2** species, is stabilized *via* H-bond with the close phenolate oxygen atom (see Fig. S1, ESI†). For this reason, as for ligand **L1**, the formation of H-bonding with the amine function leads to a decrease in its fluorescence.

This H-bond interaction, which is also monitorable through the UV-Vis spectra (see Fig. 5(b)), is also highlighted by the change in the maximum of the absorption and emission wavelengths (Fig. 5(a)) as a function of pH. λ_{max} and λ_{em} shifted in different directions, increasing the Stokes shift when the phenol becomes phenolate (pH $\geq$ 5, λ_{max} and λ_{em} shift towards lower and higher energies, respectively), while an opposite trend was observed at higher pH values (λ_{max} and λ_{em} shift towards higher and lower energies, respectively) with the formation of the neutral zwitterionic **L2** species in which a strong H-bond between the closest tertiary ammonium and phenolate groups was suggested. Taking into account the trend and shift in both λ_{max} and λ_{em}, it can be suggested that the fluorescence is yielded by light emission decay from the phenolate excited state of all **L2** species to different ground states, characterized by the formation of strong intramolecular H-bonds.

In conclusion, although **L1** is a much more efficient fluorescent system than **L2** (Table 1), both ligands show fluorescence emission depending on the protonation state of the aromatic functions. In particular, the highest emitting species are due to the monodeprotonated form of BPH of **L1** as well as to the phenolate species of PH of **L2**, both of which are achieved in the H_3L^{3+} species; on the contrary, the neutral BPH and PH species are very low fluorescence emitters. The presence of the closer tertiary amine function affects the emission quantum yield in some species by forming intramolecular H-bonding with the close phenol oxygen atom of both systems. The H-bonding induces a nonradiative relaxation process of the excited species, yielding a decrease in the fluorescence in both ligands. This H-bonding is weaker in **L1** *via* OH···N as well as $O^-\cdots HN^+$, and for this reason only a relatively low efficiency of fluorescence quenching could be observed, while it takes place strongly *via* $O^-\cdots HN^+$ in **L2** giving an almost total quenching of the fluorescence of **L2**. Taking into account these results, both ligands behave as chemosensors of H^+ in that they are able to change their optical absorption and fluorescence properties as a function of pH.

Coordination of Zn(II)

The coordination behaviour of both systems towards Zn(II) was potentiometrically studied and the results obtained are reported in ref. 25 and 31; as for basicity, the Zn(II)/**L2** system had been studied in NMe_4Cl ionic medium,[31] thus we performed new potentiometric measurements to obtain the stability constants for the Zn(II)/**L2** system under the same experimental conditions as the Zn(II)/**L1** system (0.15 mol dm^{-3} NaCl aqueous solution at 298.1 K). The potentiometrically determined stability constants for the equilibrium reactions of **L2** with Zn(II) are reported in Table 2. The species formed as well as the values of the stability constants evaluated are similar to those previously reported and thus the discussion can be outlined in the same way. The main difference found was the formation of the $[Zn_2(H_{-1}$**L2**$)(OH)_2]^+$ species in this ionic medium which was not previously detected. The addition of the second OH^- anion to $[Zn_2(H_{-1}$**L2**$)OH]^{2+}$ is quite high ($\log K$ = 3.76) suggesting that it is probably bound in a bridge disposition between the Zn(II) ions. The distribution diagrams for the Zn(II)-complexed species for both 2Zn(II)/L systems are reported in Fig. 6 for **L1** and in Fig. 8 for **L2** as a function of pH. However, the results previously discussed can be summarized in this way: (i) the dinuclear species are prevalent in solution and the only species existing at pH higher than 7 is a L/Zn(II) with a 1:2 molar ratio; (ii) the most prevalent species

 This journal is © The Royal Society of Chemistry and the Centre National de la Recherche Scientifique 2009

Published on 31 October 2008 on http://pubs.rsc.org | doi:10.1039/B810228G
Downloaded on 02 January 2013

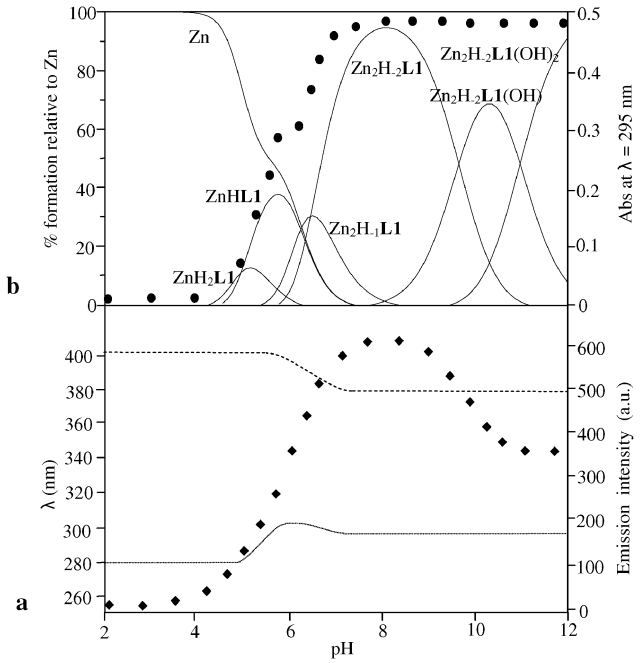

Fig. 6 Fluorescence emission titration (λ_{ex} = 283 nm) (◆), absorption wavelength trend (···), and emission wavelength trend (---) (a); absorption titration at λ = 295 nm (●) and distribution curves of the species (–) (b); as a function of pH in aqueous solution: [**L1**] = 5.0×10^{-5} M, [Zn(II)] = 10^{-4} M, I = 0.15 M NaCl, T = 298.1 K.

are $[Zn_2(H_{-2}\mathbf{L1})]^{2+}$ and $[Zn_2(H_{-1}\mathbf{L2})]^{3+}$ for **L1** and **L2**, respectively; (iii) these dinuclear species have similar molecular skeletons indicating a preorganized dinuclear Zn(II) species in which the two Zn(II), similarly coordinated, can cooperate in binding suitable guests (see Scheme 1).

Fluorescence and UV-Vis of the 2Zn(II)/L1 system at different pH values. Emission and absorption spectra were performed at different pH values using Zn(II)/**L1** at a 2 to 1 molar ratio. The trend in fluorescence emission intensity (◆) *versus* pH (λ_{exc} = 283 nm) is reported in Fig. 6(a) together with the maximum absorption (···) and emission (---) wavelength trends. Fig. 6(b) reports the trend for the absorption titration at λ = 295 nm (●) together with the distribution curves for the species of the 2Zn(II)/**L1** system (—) as a function of pH. Moreover, fluorescence titration was carried out by adding increasing amounts of Zn(II) to a HEPES buffer (pH = 7.4) solution of **L1** and the spectra are reported in Fig. 7. The fluorescence quantum yield of the highly emitting species is reported in Table 1.

The UV-Vis absorption spectra of solutions containing 2Zn(II)/**L1** recorded at different pH values were discussed previously;[25a] they showed spectral profiles indicating the deprotonation of BPH and simultaneous coordination of the Zn(II) ions; in these new experiments, some further aspects can be discussed. The absorption λ_{max} shifts toward lower energy when monitored from acidic (free ligand) to basic pH values (Zn(II)-complexes); up to the presence in solution of the Zn(II)-mononuclear species it moves from 280 to 305 nm, while the appearance in solution of the dinuclear species, at approximately pH 6, gives rise to a change in the λ_{max} which shifts from 305 nm in the presence of the mononuclear $[Zn(H\mathbf{L1})]^{3+}$ species to 298 nm with the complete formation of the more stable $[Zn_2(H_{-2}\mathbf{L1})]^{2+}$ species at pH = 7.4. This λ_{max} is preserved also at higher pH values where only dinuclear Zn(II)-complexed species are present in solution. The shift in λ_{max} observed from the mono- to the di-nuclear species can be ascribed to the full deprotonation of BPH which loses both acidic hydrogen atoms in the Zn(II)-dinuclear species, affording the bi-negative form of BPH; this result is in agreement with the studies previously reported for the Zn(II)-dinuclear species of **L1**. The changes in absorption from the mono-negative BPH to the bi-negative species are also visible in Fig. 6(b), where a change in absorptivity can also be observed when the dinuclear species appear in solution. These changes are in agreement with a change in the protonation degree of BPH and thus to its full deprotonation and simultaneous coordination of each Zn(II) ion by one phenolate oxygen atom of the BPH unit as already reported. The fluorescence experiments gave rise to analogous results, with fluorescence increasing at values starting from acidic pH and reaching maximum intensity in the field of pH 7.4–8.4 with the maximum presence in solution of the $[Zn_2(H_{-2}\mathbf{L1})]^{2+}$ species, then decreasing at higher pH values and reaching a plateau at pH > 11 with the presence in solution of the di-hydroxylated $[Zn_2(H_{-2}\mathbf{L1})(OH)_2]$ species (Fig. 6). It is interesting to note that, unlike the free **L1**, the λ_{em} changes (λ_{exc} = 283 nm) by changing the pH, and as in the absorption experiments the change occurs at the pH values where there is the formation of the Zn(II)-dinuclear species. Specifically, λ_{em} shifts from 403 nm (free ligand) to 379 nm with the formation of the $[Zn_2(H_{-2}\mathbf{L1})]^{2+}$ species, while remaining constant in the other dinuclear species. Once again, this trend can be related to the full deprotonation of BPH, as retrieved in the crystal structure of the $[Zn_2(H_{-2}\mathbf{L1})(H_2O)_2]^{2+}$ previously reported, which produces changes in the ground as well as in the excited state of BPH. Moreover, the formation of the hydroxylated $[Zn_2(H_{-2}\mathbf{L1})OH]^{+}$ and $[Zn_2(H_{-2}\mathbf{L1})(OH)_2]$ species produces a drop in fluorescence emission without changing the λ_{em} (Fig. 6(a)); this is due to an increase in electron density

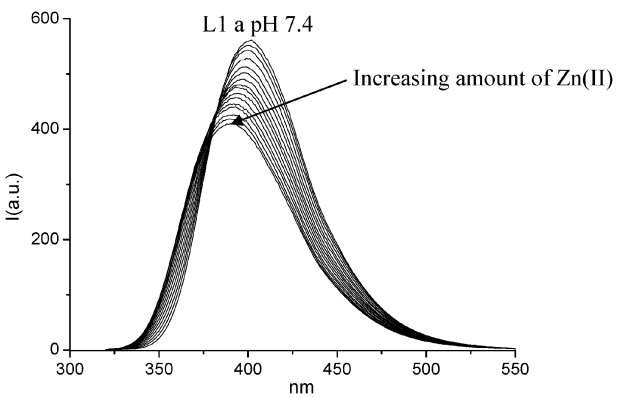

Fig. 7 Fluorescence spectra of the Zn(II)/**L1** system in aqueous buffer (HEPES, 5×10^{-2} M) solution at pH = 7.4, obtained by adding several amounts of Zn(II) up to 2 equivalents with respect to [**L1**] = 5.0×10^{-5} M.

Published on 31 October 2008 on http://pubs.rsc.org | doi:10.1039/B810228G
Downloaded on 02 January 2013

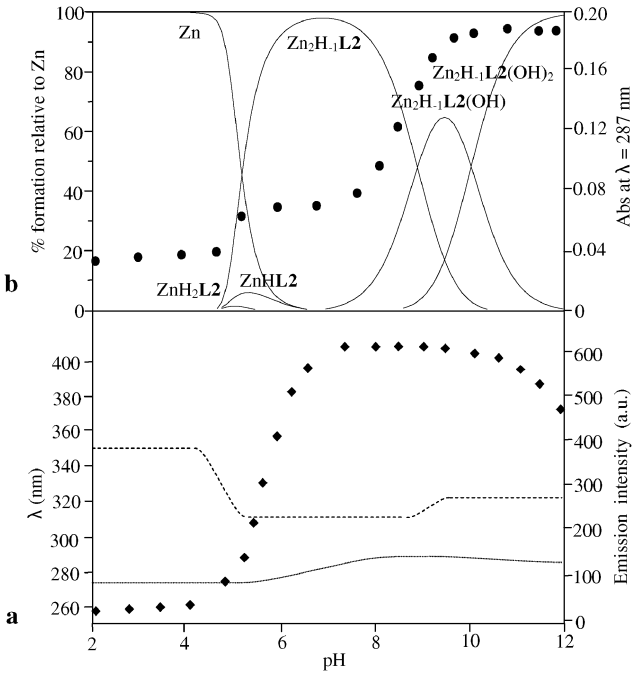

Fig. 8 Fluorescence emission titration (λ_{ex} = 279 nm) (◆), absorption wavelength trend (···), and emission wavelength trend (---) (a); absorption titration at λ = 287 nm (●) and distribution curves of the species (—) (b); as a function of pH in aqueous solution: [**L2**] = 5.0×10^{-5} M, [Zn(II)] = 1.0×10^{-4} M, I = 0.15 M NaCl, T = 298.1 K.

of the BPH unit by coordinating the OH^- species which, as reported in similar cases, increases a thermal relaxation negatively affecting emission decay mechanisms.[20b] The change in λ_{em} occurring with the formation of the dinuclear $[Zn_2(H_{-2}\mathbf{L1})]^{2+}$ is well highlighted by titrating a buffer (pH = 7.4) solution of **L1**, adding increasing amounts of Zn(II) up to 2 equivalents (Fig. 7); as shown in the figure, the λ_{em} shifts toward higher energy by adding Zn(II) but, at the same time, the fluorescence of the new species formed decreases by about 30% and thus none chelation-enhanced fluorescence (CHEF) effects were observed for this system.

Fluorescence and UV-Vis of the 2Zn(II)/L2 system at different pH values. Analogous fluorescence and absorption experiments were performed at different pH values using Zn(II)/**L2** at a 2 to 1 molar ratio; the results are reported in Fig. 8.

UV-Vis absorption spectra of solutions containing 2Zn(II)/**L2** at different pH values show, as previously reported, spectral profiles due to the deprotonated form of PH. However, also in this case, some further aspects can be discussed. Observing the λ_{max} of the spectra from acidic to alkaline pH values (Fig. 8(a)), a shift in the λ_{max} from 273 (free ligand) to 286 nm (complexed ligand) occurs at pH > 5 with the appearance in solution of the $[Zn_2(H_{-1}\mathbf{L2})]^{3+}$ species, in agreement with the deprotonation of PH as previously demonstrated. The value of λ_{max} 286 nm is enough preserved also at higher pH values where only a little decrease is shown with the appearance in solution of the dihydroxylated species (λ_{max} = 282 at pH = 12). On the contrary, in the 6–8 pH range, where the $[Zn_2(H_{-1}\mathbf{L2})]^{3+}$ species is prevalent in solution, a slight increase in absorption with respect to the free ligand can be observed, while a marked increase is visible at higher pH values with the formation of the hydroxylated $[Zn_2(H_{-1}\mathbf{L2})OH]^{2+}$ species (see Fig. 8). This finding could be explained by a different disposition of **L2** in forming the Zn–O–Zn cluster system (O is the phenolate oxygen atom) in the $[Zn_2(H_{-1}\mathbf{L2})]^{3+}$ and $[Zn_2(H_{-1}\mathbf{L2})OH]^{2+}$ species. In fact, while it was demonstrated that the hydroxylated $[Zn_2(H_{-1}\mathbf{L2})OH]^{2+}$ species shows the OH^- displaced in a bridged disposition between the two Zn(II) ions,[30] on the contrary, a coordination environment without secondary bridging ligands could be hypothesized in the $[Zn_2(H_{-1}\mathbf{L2})]^{3+}$ species. In the latter, the fifth coordination site of each Zn(II) ion could be saturated by a water molecule or by a chloride anion of the ionic medium. This may be the reason for the increase in absorption of the $[Zn_2(H_{-1}\mathbf{L2})OH]^{2+}$ with respect to the $[Zn_2(H_{-1}\mathbf{L2})]^{3+}$ species.

Analysis of the fluorescence experiments gives additional information; examining the maximum of λ_{em} (λ_{exc} = 275 nm) from acidic to alkaline field of pH, a shift of the λ_{em} is observable (see Fig. 8) at pH > 5; λ_{em} moves from 354 nm, typical of the free ligand, reaching a constant value (308 nm) at pH 6, with the full formation of the $[Zn_2(H_{-1}\mathbf{L2})]^{3+}$ species. This change in λ_{em} is coupled with an increase in fluorescence, which shows its highest emission in the range of the $[Zn_2(H_{-1}\mathbf{L2})]^{3+}$ species. These changes are in agreement with the simultaneous deprotonation of the phenolic oxygen atom due to the Zn(II) complex formation and its bridging coordination between the two Zn(II) ions, as phenolate. At pH > 9, a further change in the λ_{em} can be highlighted, since it shifts from 308 to 325 nm in concomitance with the appearance of the $[Zn_2(H_{-1}\mathbf{L2})OH]^{2+}$ species in solution; this occurs without observing any significant change in fluorescence intensity. This result may be related, as above, to a different disposition of the secondary ligands in the two complexed $[Zn_2(H_{-1}\mathbf{L2})]^{3+}$ and $[Zn_2(H_{-1}\mathbf{L2})OH]^{2+}$ species that could be responsible of the different λ_{em} in the dinuclear $[Zn_2(H_{-1}\mathbf{L2})]^{3+}$ and $[Zn_2(H_{-1}\mathbf{L2})OH]^{2+}$ species. As previously discussed for the $[Zn_2(H_{-2}\mathbf{L1})(OH)_2]$ species, the increase in the total electron density of the complex in the dihydroxylated $[Zn_2(H_{-1}\mathbf{L2})(OH)_2]^+$ species affects fluorescence at higher pH values.

The Zn(II)-**L2** dinuclear complexes showed very interesting fluorescent properties; in fact, although free **L2** exhibits emitting species in the same range of pH of the Zn(II)-dinuclear one, the fluorescence intensity of the latter is higher, giving a strong CHEF effect. This effect, occurring to **L2** in the presence of Zn(II), is highlighted in Fig. 9, which reports the fluorescence spectra of **L2** obtained by adding several amounts of Zn(II) in aqueous buffer pH = 7.4 solution. At this pH value, the species formed in the presence of Zn(II) is the $[Zn_2(H_{-1}\mathbf{L2})]^{3+}$ species. As can be observed in Fig. 9, the free ligand shows low fluorescence emission with a λ_{em} centered at 347 nm; by adding Zn(II), the emission increases and λ_{em} shifts toward higher energy. The spectra preserve the same profile when adding up to 2 equivalents of Zn(II), reaching a constant emission and λ_{em} of 308 nm, in concomitance with the complete formation of the $[Zn_2(H_{-1}\mathbf{L2})]^{3+}$ species.

 This journal is © The Royal Society of Chemistry and the Centre National de la Recherche Scientifique 2009

View Article Online

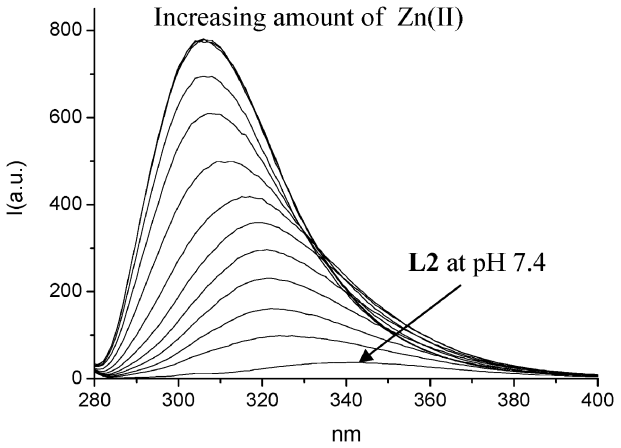

Fig. 9 Fluorescence spectra of the Zn(II)/**L2** system in aqueous buffer (HEPES, 5×10^{-2} M) solution at pH = 7.4, obtained by adding several amounts of Zn(II) up to 2 equivalents with respect to [**L2**] = 5.0×10^{-5} M.

(see Fig. 8(b)). At this pH the emission quantum yield is more than twenty-fold higher for the $[Zn_2(H_{-1}\mathbf{L2})]^{3+}$ species than for the free ligand; furthermore, a similar CHEF effect was also found in other fields of pH such as 8 and 10, at which the dinuclear species are formed, thus highlighting the sensing role of **L2** towards Zn(II) in aqueous solution in a biologically important range of pH. For this reason, **L2** can be considered a potential chemosensor for Zn(II).

Conclusions

The studies highlighted that the intensity of the fluorescence of both ligands depends on the protonation state of the phenolic functions, and in the case of **L2**, the λ_{em} is also affected by protonation while this does not occur for **L1**. For this behavior, both ligands are suitable chemosensors of H^+ in that they are able to change their optical absorption and fluorescence properties as function of pH.

For both systems the most fluorescent species is the same: H_3L^{3+} in which the BPH unit of **L1** is in its mono-deprotonated form, while PH is present as phenolate form in **L2**; on the contrary, when BPH and PH are in their neutral form both ligands show the lowest fluorescence. While these results are in agreement with those found for free BPH (the more fluorescent species is the monoanionic species of BPH), this finding is opposite to that for free PH where the neutral species is the most fluorescent. This can be explained by a lower solvation of the phenolate oxygen atom in the $H_3\mathbf{L2}^{3+}$ species which limits the quenching effect occurring *via* H-bond with the water molecules. The presence of the tertiary amine function close to the phenol oxygen affects the emission quantum yield of those species in which the formation of intramolecular H-bonds is possible, highlighting that the formation of H-bonds has a quenching effect to the fluorescence in these systems.

The Zn(II)-dinuclear species are fluorescent in the field of pH where they exist; the highest emitting species are the $[Zn_2(H_{-2}\mathbf{L1})]^{2+}$ and the $[Zn_2(H_{-1}\mathbf{L2})]^{3+}$ species, respectively; they are prevalent in a wide range of pH including the physiological one. In the $[Zn_2H_{-2}\mathbf{L1}]^{2+}$, the presence of the dianionic form of BPH produces a blue shift of λ_{em} in the fluorescence experiments, in comparison with the free ligand. The interaction with guests such as OH^- perturbs the emission but not the absorption of the dinuclear species.

In the $[Zn_2(H_{-1}\mathbf{L2})]^{3+}$ species a slight blue shift in λ_{em} can also be observed, as well as, a decrease in fluorescence brought about by the addition of an anionic guest such as OH^-.

The main result retrieved is that both **L1** and **L2** sense the Zn(II) in aqueous solution at physiological pH 7.4 by fluorescence; at this pH the $[Zn_2(H_{-2}\mathbf{L1})]^{2+}$ and $[Zn_2(H_{-1}\mathbf{L2})]^{3+}$ species are prevalent in solution. The $[Zn_2(H_{-2}\mathbf{L1})]^{2+}$ species shows a simultaneous change in the λ_{em} with a drop in fluorescence, but real and efficient sensing was obtained by using ligand **L2** which, in the presence of two equivalents of Zn(II), gives rise to a strong CHEF effect (a twenty-fold increase) with the formation of the $[Zn_2(H_{-1}\mathbf{L2})]^{3+}$ species; in this case, a similar CHEF effect was also found in other fields of pH such as 8 and 10, highlighting the sensing role of **L2** towards Zn(II) in aqueous solution in a biologically important range of pH.

Concluding, both systems behave as chemosensors for both H^+ and Zn(II) and their investigation has given much useful information for the design of more efficient systems. Moreover, taking into account that both $[Zn_2(H_{-2}\mathbf{L1})]^{2+}$ and $[Zn_2(H_{-1}\mathbf{L2})]^{3+}$ dinuclear species show the highest fluorescence intensity and that they are the most suitable hosting species for guests, they are a very interesting platform for the sensing of guest species.

Acknowledgements

The authors thank the Italian Ministero dell'Istruzione dell'Università e della Ricerca (MIUR), PRIN2007 for financial support.

References

1 (*a*) *Fluorescent Chemosensors of Ion and Molecule Recognition*, eds. J.-P. Desvergne and A. W. Czarnik, NATO-ASI Series, Kluwer Academic Publishers, 1996; (*b*) U. E. Spichiger-Keller, *Chemical Sensors and Biosensors for Medical and Biological Applications*, Wiley-VCH, 1998; (*c*) *Fluorescent Chemosensors for Ion and Molecule Recognition*, ed. A. W. Czarnik, ACS, Washington, DC, 1992.
2 (*a*) *Chem. Rev.*, 2000, **100**, 2477–2738, special issue on Chemical Sensors, eds. A. B. Ellis and D. R. Walt; (*b*) *Coord. Chem. Rev.*, 2000, **205**, 1–232, special issue on luminescent sensors, ed. L. Fabbrizzi; (*c*) special issue on synthetic receptors as sensors, ed. A. V. Aslin, *Tetrahedron*, 2004, **60**, 11055–11316.
3 (*a*) Special issue on luminescent sensors, eds. A. P. deSilva and P. Tecilla, *J. Mater. Chem.*, 2005, **15**, 2617–2976; (*b*) A. P. de Silva, G. D. McClean, T. S. Moody and S. M. Weir, in *Handbook of Photochemistry and Photobiology*, ed. H. S. Nalwa, American Institute of Physics, 2003, vol. 3, p. 217.
4 L. Fabbrizzi, M. Licchelli and A. Taglietti, *Dalton Trans.*, 2003, 3471.
5 K. Rurack, *Spectrochim. Acta, Part A*, 2001, **57**, 2161.
6 R. Martinez-Manez and F. Sancenon, *Chem. Rev.*, 2003, **103**, 4419.
7 (*a*) K. J. Albert, N. S. Lewis, C. L. Schauer, G. A. Sotzing, S. E. Stitzel, T. M. Vaid and D. R. Walt, *Chem. Rev.*, 2000, **100**, 2595; (*b*) W. Göpel, *Sens. Actuators B*, 1998, **52**, 125; (*c*) J. J. Lavigne and E. V. Anslyn, *Angew. Chem., Int. Ed.*, 2001, **40**, 3118; (*d*) A. D'Amico, C. Di Natale and R. Paolesse, *Sens. Actuators B*, 2000, **68**, 324.

Published on 31 October 2008 on http://pubs.rsc.org | doi:10.1039/B810228G
Downloaded on 02 January 2013

View Article Online

8 (*a*) L. Prodi, F. Bolletta, M. Montalti and N. Zaccheroni, *Coord. Chem. Rev.*, 2000, **205**, 59; (*b*) C. Bargossi, M. C. Fiorini, M. Montalti, L. Prodi and N. Zaccheroni, *Coord. Chem. Rev.*, 2000, **208**, 17–32; (*c*) L. Prodi, *New J. Chem.*, 2005, **29**, 20.

9 (*a*) *"Advanced Concepts in Fluorescent sensing, Part A: Small Molecule Sensing"*, in *Topics in Fluorescence Spectroscopy*, vol. 9; (*b*) *"Advanced Concepts in Fluorescent sensing, Part B: Macromolecular Sensing"*, eds. C. D. Geddes and J. R. Lakowicz, Springer, 2005, vol. 10.

10 J. R. Lakowicz, *Principles of Fluorescence Spectroscopy*, Kluwer Academic/Plenum Publishers, 1999.

11 R. Y. Tsien, *Annu. Rev. Neurosci.*, 1989, **12**, 227.

12 A. P. de Silva, H. Q. N. Gunaratne, T. Gunnlaugsson, A. J. M. Huxley, C. P. McCoy, J. T. Rademacher and T. E. Rice, *Chem. Rev.*, 1997, **97**, 1515.

13 Special Issue on Chemical sensors, guest editors A. B. Ellis and D. R. Walt, *Chem. Rev.*, 2000, **100**, 2477–2738.

14 K. Rurack, *Spectrochim. Acta, Part A*, 2001, **57**, 2161.

15 L. Fabbrizzi, M. Licchelli and A. Taglietti, *Dalton Trans.*, 2003, 3471.

16 W. T. Bell and N. M. Hext, *Chem. Soc. Rev.*, 2004, **33**, 589.

17 (*a*) L. Prodi, *New J. Chem.*, 2005, **29**, 20; (*b*) G. Farrugia, S. Iotti, L. Prodi, M. Montalti, N. Zaccheroni, P. B. Savage, V. Trapani, P. Sale and F. I. Wolf, *J. Am. Chem. Soc.*, 2006, **128**, 344–350; (*c*) G. Farrugia, S. Iotti, L. Prodi, N. Zaccheroni, M. Montalti, P. Savage, G. Andreani, V. Trapani and F. I. Wolf, *J. Fluorescence*, DOI: 10.1007/s10895-008-0374-6; (*d*) M. Montalti, L. Prodi and N. Zaccheroni, *J. Mater. Chem.*, 2005, **15**, 2810–2814.

18 Theme Issue: Fluorescent Sensors, *J. Mater. Chem.*, 2005, **15**, 2617–2976.

19 L. Basade-Desmonts, D. N. Reinhoudt and M. Crego-Calama, *Chem. Soc. Rev.*, 2007, **36**, 993.

20 (*a*) J. W. Bridges, P. J. Creaven and R. T. Wiliams, *Biochem. J.*, 1965, **96**, 872; (*b*) J. Mohanty, H. Pal and A. V. Sapre, *Bull. Chem. Soc. Jpn.*, 1999, **72**, 2193.

21 (*a*) J. Feitelson, *J. Phys. Chem.*, 1964, **68**, 691; (*b*) M. Krauss, J. O. Jensen and H. F. Hameka, *J. Phys. Chem.*, 1994, 9955.

22 (*a*) J. E. Coleman, in *Zinc Enzymes*, Birkauser, Boston, MA, 1986, ch. 4, pp. 49–58; (*b*) Lindskog, in *Zinc Enzymes*, Birkauser, Boston, MA, 1986, ch. 22, pp. 307–316; (*c*) E. Erksson, T. A. Jones and A. Liljas, in *Zinc Enzymes*, Birkauser, Boston, MA, 1986, ch. 23, pp. 317–328; (*d*) A. C. Sen, C. K. Tu, H. Thomas, G. C. Wynns and Silvermann, in *Zinc Enzymes*, Birkauser, Boston, MA, 1986, ch. 24, pp. 329–340; (*e*) Y. Pocker, N. Janjic and C. H. Miao, in *Zinc Enzymes*, Birkauser, Boston, MA, 1986, ch. 25, pp. 341–356; (*f*) R. G. Khalifah, J. I. Rogers and J. Mukherjee, in *Zinc Enzymes*, Birkauser, Boston, MA, 1986, ch. 26, pp. 357–370.

23 J. M. Berg and Y. Shi, *Science*, 1996, **271**, 1081.

24 (*a*) P. Jiang and Z. Guo, *Coord. Chem. Rev.*, 2004, **248**, 205; (*b*) S. C. Burdette, G. K. Walkup, B. Spingler, R. Y. Tsien and S. J. Lippard, *J. Am. Chem. Soc.*, 2001, **123**, 7831; (*c*) E. M. Nolan and S. J. Lippard, *Inorg. Chem.*, 2004, **43**, 8310; (*d*) L. Rodriquez, J. C. Lima, J. Parola, R. Meitz, R. Aucejo, E. Garcia-España, J. M. Linares, C. Soriano and J. Alarcón, *Inorg. Chem.*, 2008, **47**, 6173.

25 (*a*) G. Ambrosi, M. Formica, V. Fusi, L. Giorgi, A. Guerri, M. Micheloni, P. Paoli, R. Pontellini and P. Rossi, *Inorg. Chem.*, 2007, **46**, 309; (*b*) P. Dapporto, M. Formica, V. Fusi, M. Micheloni, P. Paoli, R. Pontellini and P. Rossi, *Inorg. Chem.*, 2000, **39**, 4663.

26 M. Fontanelli and M. Micheloni, *I Spanish–Italian Congress Thermodynamics of Metal Complexes*, Univ. of Valencia, Spain, Peñiscola, June 3–6, 1990, p. 41.

27 (*a*) G. Gran, *Analyst*, 1952, **77**, 661; (*b*) F. J. Rossotti and H. Rossotti, *J. Chem. Educ.*, 1965, **42**, 375.

28 P. Gans, A. Sabatini and A. Vacca, *Talanta*, 1996, **43**, 1739.

29 (*a*) J. N. Demas and G. A. Crosby, *J. Phys. Chem.*, 1971, **75**, 991; (*b*) M. T. Gandolfi, A. Credi, M. Montalti and L. Prodi, *Handbook of Photochemistry*, 3rd edn, CRC Press, Boca Raton, FL.

30 N. Ceccanti, M. Formica, V. Fusi, L. Giorgi, M. Micheloni, R. Pardini, R. Pontellini and M. R. Tiné, *Inorg. Chim. Acta*, 2001, **321**, 153.

31 P. Dapporto, M. Formica, V. Fusi, L. Giorgi, M. Micheloni, P. Paoli, R. Pontellini and P. Rossi, *Inorg. Chem.*, 2001, **40**, 6186.

32 (*a*) H. Pal and T. N. Das, *J. Phys. Chem.*, 2003, **107**, 5876; (*b*) M. Jonsson, J. Lind and G. Merényi, *J. Phys. Chem.*, 2002, **106**, 4758; (*c*) M. Jonsson, J. Lind and G. Merényi, *J. Phys. Chem.*, 2003, **107**, 5878.

33 (*a*) A. Testa, *J. Photochem. Photobiol. A: Chem.*, 1992, **64**, 73; (*b*) G. Wenska, B. Skalski, Z. Gdaniec, R. W. Adamiak, J. Matulic-Adamic and L. Beigelman, *J. Photochem. Photobiol. A: Chem.*, 2000, **133**, 169–176.

34 (*a*) J. C. Batchelor, J. H. Prestegard, R. J. Cushley and S. R. Lipsy, *J. Am. Chem. Soc.*, 1973, **95**, 6558; (*b*) A. R. Quirt, J. R. Lyerla, I. R. Peat, J. S. Cohen, W. R. Reynold and M. F. Freedman, *J. Am. Chem. Soc.*, 1974, **96**, 570; (*c*) J. C. Batchelor, *J. Am. Chem. Soc.*, 1975, **97**, 3410.

Published on 31 October 2008 on http://pubs.rsc.org | doi:10.1039/B810228G
Downloaded on 02 January 2013

 This journal is © The Royal Society of Chemistry and the Centre National de la Recherche Scientifique 2009